UDC 669.017:669.3 + 621.721.1
https://doi.org/10.17073/0021-3438-2023-6-66-83

Research article
Научная статья

Restoration of continuous casting machine mold copper plates made of Cr–Zr bronze using multi-pass friction stir lap welding

A.V. Makarov[1], **N.V. Lezhnin**[1], **A.B. Kotelnikov**[2], **A.A. Vopneruk**[2], **Yu.S. Korobov**[1,3], **A.I. Valiullin**[1], **E.G. Volkova**[1]

[1] **M.N. Mikheev Institute of Metal Physics of Ural Branch of Russian Academy of Sciences**
18 S. Kovalevskaya Str., Yekaterinburg 620108, Russia

[2] **R&D Enterprise "Mashprom"**
5 Krasnoznamennaya Str., Yekaterinburg 620143, Russia

[3] **Ural Federal University named after the First President of Russia B.N. Yeltsin**
19 Mira Str., Yekaterinburg 620002, Russia

✉ Alexey V. Makarov (av-mak@yandex.ru)

Abstract: An innovative technology has been developed and implemented for the restoration and manufacturing of new mold copper plates for continuous casting machines (CCMs) using wear-resistant composite coatings. These copper plates significantly surpass the service life of imported copper plates featuring galvanic coatings, sometimes by up to 20 times. However, the pressing challenge of restoring the copper plates of molds once they have reached the minimum permissible thickness remains unresolved. This study aimed to explore the feasibility of restoring a plate composed of precipitation-hardening Cr–Zr bronze with the same material by employing friction stir lap welding (FSLW). The objectives were to examine the structure, quality, and hardness of the welded joint, alongside investigating the impact of heat treatment (quenching and aging). By utilizing multi-pass FSLW method with a rotating tool crafted from a heat-resistant alloy and overlapping (partially overlapping) successive passes, a welded joint with a thickness of ~5 mm was achieved, devoid of critical continuity flaws (cracks or voids). Within the bronze layer restored through FSW, a softening effect ranging from 85–105 HV1 was observed compared to the initial hardness of the bronze in its hardened and aged state while in service (116–126 HV1). This is attributed to recrystallization and overaging, specifically the coarsening of chromium particles within the Cr–Zr bronze due to the heating of the weld nugget (stir zone) to 600–700 °C. The observed softening effect during FSW can be effectively rectified through heat treatment involving dissolution of the hardening phases followed by aging, resulting in a hardness increase to approximately 120–150 HV1. The process of restoring copper plates to their original thickness via the progressive and environmentally friendly FSW method, followed be the subsequent application of wear-resistant composite coatings, presents the opportunity for an almost infinite operational cycle of molds. This advancement could potentially eradicate the necessity for Russia to rely on importing such molds copper plates.

Keywords: mold copper plate, restoration, bronze, friction stir lap welding (FSLW), hardness, structure, hardening, aging.

Acknowledgments: This research received support from the Ministry of Science and Higher Education of the Russian Federation (Research topic "Structure" No. 122021000033-2) and from the integrated project titled "Development of new materials and technologies for the formation of coatings resistant to abrasive and corrosive wear" (Ural Interregional Research and Education Center for Advanced Production Technologies and Materials). The work used equipment from the Shared Use Center "Testing Center for Nanotechnologies and Advanced Materials" (Institute of Physics and Mathematics, Ural Branch, Russian Academy of Sciences).

For citation: Makarov A.V., Lezhnin N.V., Kotelnikov A.B., Vopneruk A.A., Korobov Yu.S., Valiullin A.I., Volkova E.G. Restoration of continuous casting machine mold copper plates made of Cr–Zr bronze using multi-pass friction stir lap welding. *Izvestiya. Non-Ferrous Metallurgy.* 2023;29(6):66–83. https://doi.org/10.17073/0021-3438-2023-6-66-83

Восстановление стенок кристаллизаторов машин непрерывного литья заготовок из хромоциркониевой бронзы методом многопроходной сварки трением с перемешиванием

А.В. Макаров[1], **Н.В. Лежнин**[1], **А.Б. Котельников**[2], **А.А. Вопнерук**[2], **Ю.С. Коробов**[1,3], **А.И. Валиуллин**[1], **Е.Г. Волкова**[1]

[1] **Институт физики металлов им. М.Н. Михеева УрО РАН**
Россия, 620108, г. Екатеринбург, ул. С. Ковалевской, 18

[2] **ЗАО «НПП “Машпром”»**
Россия, 620143, г. Екатеринбург, ул. Краснознамённая, 5

[3] **Уральский федеральный университет имени первого Президента России Б.Н. Ельцина**
Россия, 620002, г. Екатеринбург, ул. Мира, 19

✉ Алексей Викторович Макаров (av-mak@yandex.ru)

Аннотация: Разработана и практически реализована инновационная технология восстановительного ремонта и производства новых стенок кристаллизаторов машин непрерывного литья заготовок (МНЛЗ) с износостойкими композиционными покрытиями, значительно (до 20 раз) превосходящих ресурс импортных стенок с гальваническими покрытиями. Однако нерешенной остается актуальная задача восстановления медных стенок (плит) кристаллизаторов после достижения ими минимально допустимой толщины. Целью работы являлось исследование возможности восстановления плиты из дисперсионно-твердеющей хромоциркониевой бронзы марки БрХЦр этим же материалом с использованием сварки трением с перемешиванием (СТП), изучение структуры, качества и твердости сварного соединения, а также влияния на его структуру и твердость термической обработки (закалки и старения). С применением многопроходной плоскостной СТП вращающимся инструментом из жаропрочного сплава при наложении (частичном перекрытии) последовательных дорожек получено сварное соединение толщиной ~5 мм без критичных дефектов сплошности (трещин, пор). В восстановленном способом СТП слое бронзы обнаружено разупрочнение до 85–105 HV1 по сравнению с исходной твердостью бронзы в закаленном и состаренном состоянии плиты, бывшей в эксплуатации (116–126 HV1). Это связано с рекристаллизацией и перестариванием (укрупнением частиц хрома) в Cr–Zr-бронзе в результате нагрева ядра сварки (зоны перемешивания) до температур 600–700 °С. Отмеченное разупрочнение при СТП может быть эффективно устранено термической обработкой (закалкой с последующим старением), приводящей к повышению твердости до 120–150 HV1. Восстановление медных плит до первоначальной толщины прогрессивным экологичным методом СТП с последующим нанесением износостойких композиционных покрытий открывает перспективы практически бесконечного цикла эксплуатации кристаллизаторов и исключения потребности России в их импорте.

Ключевые слова: плита кристаллизатора, восстановительный ремонт, бронза, сварка трением с перемешиванием (СТП), твердость, структура, закалка, старение.

Благодарности: Работа выполнена в рамках государственного задания Минобрнауки России (тема «Структура», № 122021000033-2) и комплексного проекта «Разработка новых материалов и технологий для формирования покрытий, стойких в условиях абразивного и коррозионного изнашивания» УМНОЦ мирового уровня «Передовые производственные технологии и материалы». Работа выполнена с использованием оборудования ЦКП «Испытательный центр нанотехнологий и перспективных материалов» ИФМ УрО РАН.

Для цитирования: Макаров А.В., Лежнин Н.В., Котельников А.Б., Вопнерук А.А., Коробов Ю.С., Валиуллин А.И., Волкова Е.Г. Восстановление стенок кристаллизаторов машин непрерывного литья заготовок из хромоциркониевой бронзы методом многопроходной сварки трением с перемешиванием. *Известия вузов. Цветная металлургия*. 2023;29(6):66–83.
https://doi.org/10.17073/0021-3438-2023-6-66-83

Introduction

Continuous casting machines (CCMs) (Fig. 1, *a*) contribute to more than 96 % of global steel production [1]. The main technological component of the CCM is the mold, wherein the crucial consumable element comprises water-cooled plates made from copper alloys (Fig. 1, *b*). To decrease wear resulting from friction with the solidifying slab shell, the thermal effects of liquid and solidifying metal, as well as corrosive wear of the copper plates in the lower part of the mold [2], protective coatings are applied to the working surface of these copper plates.

The dependency on imported copper plates featuring protective galvanic coatings in Russian metallurgical plants was notably high, reaching 97 % in 2012. This heavy reliance is critical for Russian national safety. The exit of foreign manufacturers and suppliers of plates from the Russian market poses a tangible threat to the Russian steel industry. Over the period spanning from the 1960s to the 2000s, advancements in the composition of galvanic coatings led to a significant rise in the average durability of copper plates, escalating from 100 to 1000 heats [1].

Nevertheless, the imported galvanic coatings employed as protective coatings present significant drawbacks: notable susceptibility to wear and tear (Fig. 2, *a*), the occurrence of thermal cracks within the coating (Fig. 2, *b*), alongside high costs and limited environmental friendliness associated with the galvanization method.

In Russia, a collaborative endeavor involving specialists from R&D Enterprise "Mashprom", JSC, Institute of Metal Physics, Institute of Engineering Science of Ural Branch of the Russian Academy of Sciences, Ural Federal University, and several metallurgical enterprises has successfully developed and implemented an innovative technology for the restorative repair and production of new copper plates for CCM molds, integrating wear-resistant composite coatings [1; 3] (Fig. 3).

During the development of this new domestic technology, a series of pivotal tasks were addressed:

— formulation of metal-ceramic powder mixtures for wear-resistant coatings was achieved by using powders within the Ni—Cr alloying system, incorporating carbides (WC, Cr_3C_2, SiC, TiC), borides (CrB_2, TiB_2), and metallic (Cr, Mo) compounds. Additionally, a unique technology involving robotic high velocity air fuel (HVAF) thermal spraying for applying coatings was created [1; 4];

— scientific substantiation of the optimal application efficacy of composite coatings containing substantial strengthening phases was accomplished [5];

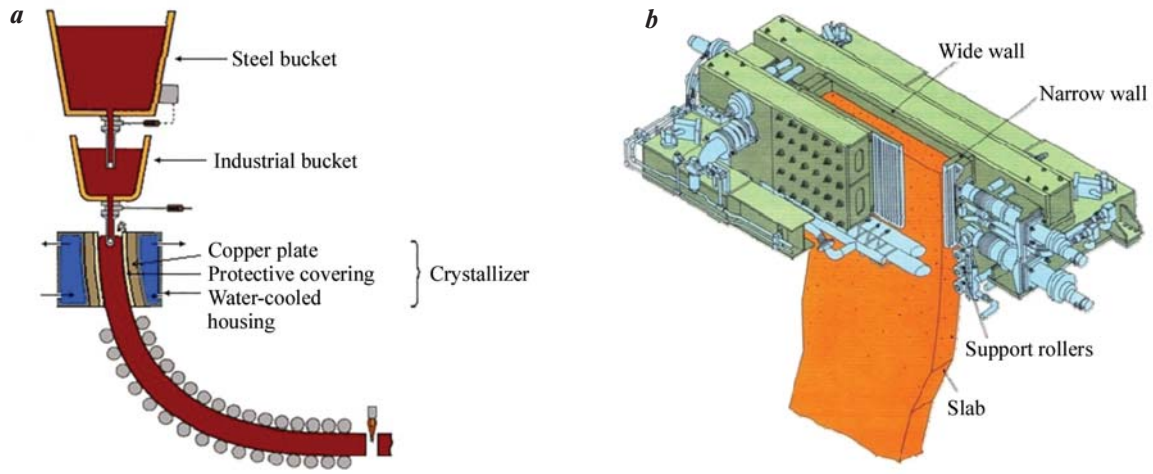

Fig. 1. Schematic view of the slab continuous casting machine (CCM) (***a***) and mold design for the slab CCM (***b***)

Рис. 1. Схема машины непрерывного литья заготовок (***a***) и конструкция кристаллизатора слябовой МНЛЗ (***b***)

Fig. 2. Electroplated coatings defects: wear (***a***) and heat cracks (***b***)

Рис. 2. Дефекты гальванических покрытий: износ (***a***) и тепловые трещины (***b***)

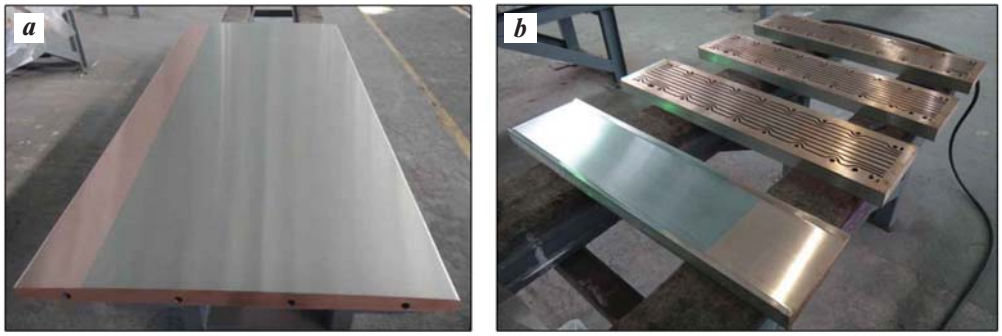

Fig. 3. Slab CCM mold plates: wide (***a***) and narrow (***b***)

Рис. 3. Широкая (***a***) и узкие (***b***) стенки кристаллизатора слябовой МНЛЗ

— a methodology was developed, enabling the reinforcement of copper alloy and enhancing the heat and wear resistance of the coating. This was achieved through the implementation of a new scientific phenomenon wherein a wear-resistant framework composed of coarse carbide and boride particles is formed during annealing [6—9].

During industrial trials conducted at Russian metallurgical enterprises such as MMK, EVRAZ NTMK, Severstal, NLMK, OMK-Steel, and others, it was determined that the durability of the innovative mold copper plates increased significantly, ranging from 4 to 20 times when compared to imported counterparts equipped with galvanic coatings. Simultaneously, these advancements led to an enhancement in the quality of produced billets. The wear resistance of the composite coatings has demonstrated an ability to endure up to 700 thousand tons of cast steel within a single overhaul cycle. The integration of this technology into the production complex of R&D Enterprise "Mashprom" in Nizhny Tagil surpasses the production capabilities of foreign companies that rely on galvanic production. This superiority extends across environmental safety, energy efficiency, and resource utilization. The development entirely aligns with the objectives outlined in the action plan of the Russian Ministry of Industry and Trade, specifically addressing the need for import substitution in heavy machine building. Following the successful implementation of this technology in major Russian Steelmakers, the proportion of foreign slab molds utilized in domestic steel mills decreased substantially, reaching 40 % by the end of 2022.

The pressing challenge of restoring copper plates in molds after reaching the minimum allowable thickness remains unresolved. When the loss of copper plate material reach 10—15 mm due to wear and repair cycles (Fig. 4), the costly plate with cooling channels is typically discarded as it no longer meets the necessary mechanical characteristic requirements.

Presently, the restoration of copper plates of continuous casting molds primarily relies on arc welding using a non-consumable electrode within inert gases (Fig. 5). However, this process exhibits low manufacturability concerning this specific product due to the metallurgical intricacies involved in welding this material. Copper and its alloys possess distinctive attributes such as high thermal conductivity, heat capacity, coefficient of thermal expansion, and a susceptibility to forming hot cracks and pores. Notably, within the temperature range of $t = 250 \div 550$ °C, copper experiences a reduction in strength and ductility [10]. These properties necessitate the preheating of a solid plate during TIG welding, within a fairly narrow temperature range of approximately 350±10 °C. Throughout the TIG welding process on a solid plate, maintaining the temperature within this narrow range proves challenging. This difficulty significantly escalates the labor intensity compared to volume-based metal deposition estimations. The constant

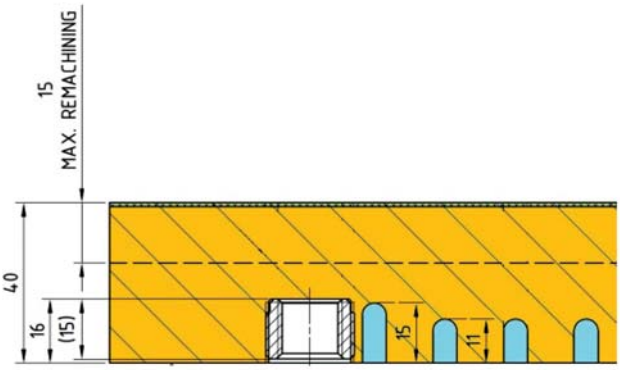

Fig. 4. Schematic diagram of the copper CCM mold plate
Dimensions in mm

Рис. 4. Конструкция медной плиты кристаллизатора МНЛЗ
Размеры указаны в мм

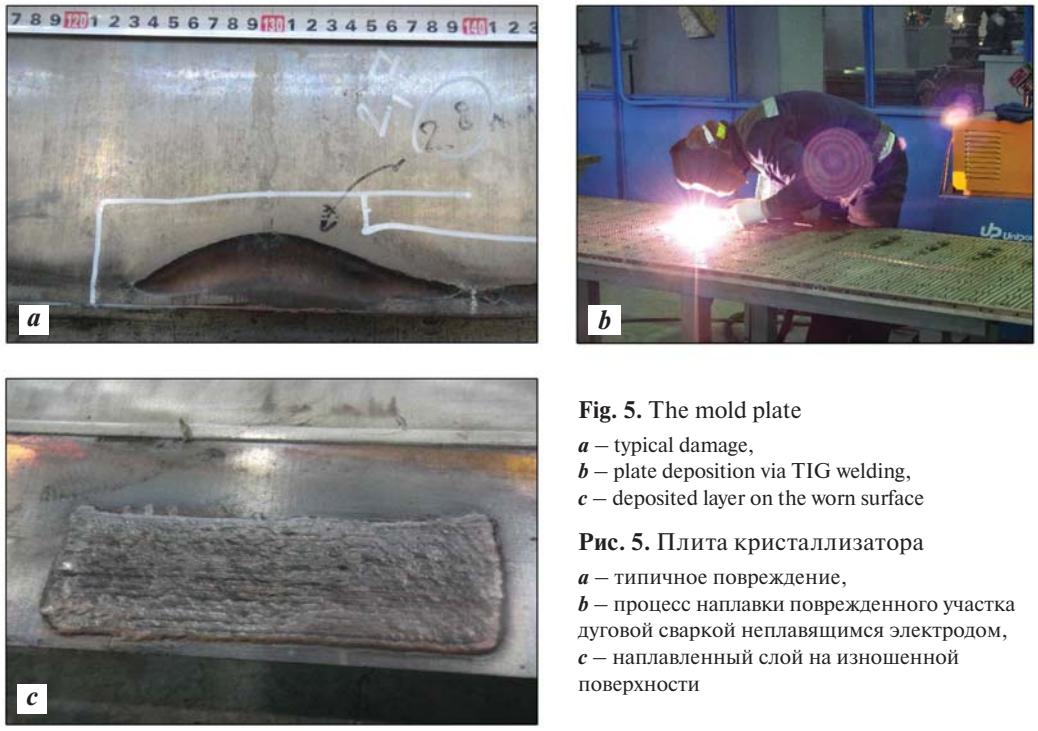

Fig. 5. The mold plate
a – typical damage,
b – plate deposition via TIG welding,
c – deposited layer on the worn surface

Рис. 5. Плита кристаллизатора
a – типичное повреждение,
b – процесс наплавки поврежденного участка дуговой сваркой неплавящимся электродом,
c – наплавленный слой на изношенной поверхности

need for plate heating, labor costs to rectify defects, and the inconsistent quality of the deposited metal amplify labor requirements. Moreover, this technology poses environmental hazards and risks to the welder's health.

Consequently, the information presented in Fig. 5 cannot be deemed a viable restoration technology for extensive surface areas of plates, let alone for full-size plates.

The utilization of specialized solid-state welding methods such as diffusion welding [11], explosion welding [12], and ultrasonic welding [13] for the aforementioned purposes is unfeasible. The impossibility of using laser techniques arises from the high reflectivity exhibited by copper (95 %) and Cu—Cr—Zr alloy (90 %) when exposed to fiber optic and other solid-state lasers emitting at a wavelength (λ) of 1064 nm, which is standard in most complexes used for laser cladding and additive manufacturing [14; 15]. This reflective property hinders the application of modern laser technologies for the restoration of copper plates. The absorption capacity of copper and chromium-zirconium bronze significantly increases only for ultrashort wavelengths (less than 550 nm) of electromagnetic radiation. However, powerful technological laser installations utilizing green (λ = 510÷532 nm) and blue (λ = 360÷÷480 nm) lasers have yet to be developed. Consequently, the restoration of copper plates of CCM molds is most promisingly addressed by advancing an environmentally friendly friction stir welding (FSW) technology to resolve these challenges.

The FSW technology, initially proposed in the Soviet Union [16] and subsequently patented by the British Institute of Welding in 1991 [17], facilitates the joining of materials in a solid state by employing a rotating tool to stir the materials. This process induces a plastic state in the material due to frictional heating without reaching a melting point, resulting in the formation of a weld through mechanical stirring of the metal in the workpieces [18—20]. FSW operates at relatively low temperatures, circumventing issues associated with conventional fusion welding, such as overheating and related crystallization defects like porosity, cast structure, and crystallization cracks. Since the early 2000s, active research has been conducted on FSW and Friction Stir Processing (FSP) of pure copper [21—23] and nickel aluminum bronze [24; 25]. Extensive studies have focused on creating dissimilar welded joints involving copper alloys [26; 27], copper or bronze in combination with other metals [28—31], and analyzing structural patterns during FSW of copper [21]. Additionally, investigations have explored phase transformations and various properties of surface-modified FSP cast nickel-aluminum bronzes, encompassing corrosion and cavitation resistance, as well as fatigue resistance [18; 32—34]. Specific studies have delved into the characteristics of FSW involving Cu—Cr—Zr alloys [35; 36].

In a study [37], the potential for restoring CCM mold copper plates using the FSW method with a Cu—Ag alloy is discussed. Moreover, research has demonstrated the capability of joining pure copper plates with thick-

nesses of 16—22 mm to copper plates with thicknesses of 2.5—5.0 mm using FSW [38]. The intricacies of FSLW of a 5 mm thick plate made of pure copper to a fragment of a mold plate, composed of Cr—Zr bronze, were examined [39]. However, it's noteworthy that in studies [37; 39], the welding was conducted in separate tracks rather than over the entire surface.

To restore substantial sections of the plate, multi-pass FSLW involving the sequential overlap of welds is necessary, subjecting the metal to thermomechanical influence during joint performance. Achieving complete restoration of a Cr—Zr bronze plate is best accomplished using the same bronze material as a filler rather than pure copper, as detailed in [38]. This study demonstrated that, under specific FSW conditions, a welded copper joint exhibited nearly equal strength compared to a copper base. When restoring Cr—Zr bronze with a pure copper plate in the welding zone, an increase in microhardness to 150—190 HV1 was observed compared to the original coarse-grained bronze with a hardness of 110—130 HV1. This rise was attributed to the formation of an ultrafine structure (0.5—1.0 μm) resulting from FSW and dispersion strengthening of the alloy using nano-sized particles of chromium and the Cu_5Zr intermetallic compound [39].

However, in the case of multi-pass FSLW of thick Cu—Cr—Zr alloy plate, high temperatures within the mixing zone led to adverse effects such as grain growth, dissolution and coarsening of strengthening phases. This resulted in a detrimental impact on the mechanical and physical properties of the material [40]. The structure and strength properties of Cr—Zr bronze can be significantly influenced by both the thermomechanical effects during multipass FSLW and subsequent heat treatment processes, particularly hardening and aging, which are commonly employed for dispersion-hardening alloys.

The objective of this study is to investigate the potential for restoring a plate made of dispersion-strengthened Cr—Zr bronze using the same material through the multi-pass friction stir lap welding method while applying consecutive joints with partial overlay. Additionally, the study aims to analyze the structure, integrity, and hardness of the welded joint, as well as to assess the impact of heat treatment (quenching and aging) on its structure and hardness.

Materials and methods

The foundational material comprised a 38 mm thick plate, constituting the copper plate of a CCM mold. Made from precipitation-hardening chromium zirconium bronze, it underwent hardening, aging, and subsequent operational phases. Additionally, a 5 mm thick bronze plate with identical chemical composition served as filler material, wt.%: 98.82—99.57 Cu; 0.80 Cr; 0.13 Zr; <0,03.Ni; <0.01 As; <0.003 Pb; <0.01 Zn; <0.002 Bi; <0.01 Sn; <0.1 impurities. Unlike solid solution strengthened alloys, which exhibit reduced thermal conductivity due to dissolved alloying elements, the precipitation-strengthened Cu—Cr—Zr alloy offers both high strength and superior thermal conductivity [41]. The remarkably low solubility of chromium and zirconium in copper at temperatures below 600 °C facilitates the creation of an alloy matrix primarily composed of pure copper, thereby ensuring high thermal conductivity. Meanwhile, finely dispersed particles of chromium and the intermetallic compound Cu_5Zr serve as strengthening phases, significantly enhancing the alloy's strength and heat resistance following thermal aging. Chromium plays an important role in dispersion strengthening, whereas zirconium contributes to elevating the recrystallization temperature, thereby enhancing heat resistance.

To bond the plates through an "overlap" technique, a portal welding setup was utilized at the Institute of Metal Physics of Ural Branch of the Russian Academy of Sciences (Fig. 6, *a*). The workpiece was secured onto the welding table using the equipment depicted in Fig. 6, *b*. For the welding process, a specialized welding tool crafted from the heat-resistant alloy was employed. This tool featured a conical threaded pin, 6 mm in length, with a base diameter of 8 mm tapering down to 6 mm at the tip (Fig. 7, *a*). As illustrated in Fig. 7, this rotating welding tool was angled at $\alpha = 3°$ opposite to the welding direction and immersed into the filler plate, thereby generating a zone of superplasticity. The heat necessary for welding was produced through the friction between the rotating tool's pin and the shoulder, combined with intense plastic deformation of the metal plate. The heating process resulted in the plasticization of the material around the pin. As the tool moved forward, it mechanically transferred the material from the front to the back edge of the tool, effectively filling the weld. The tool's shoulder applied pressure to the plate's surface, ensuring that the flow of plasticized metal remained close to it. Consequently, a welded joint was formed without requiring the material to melt.

Multi-pass lap welding was executed through a sequence of successive passes, with a seam axis step of 6 mm, which accounts for 0.86 of the average diameter of the tool's conical pin, measuring 7 mm. The welding parameters were as follows: load $S = 13.7 \div 15.7$ kN, spindle

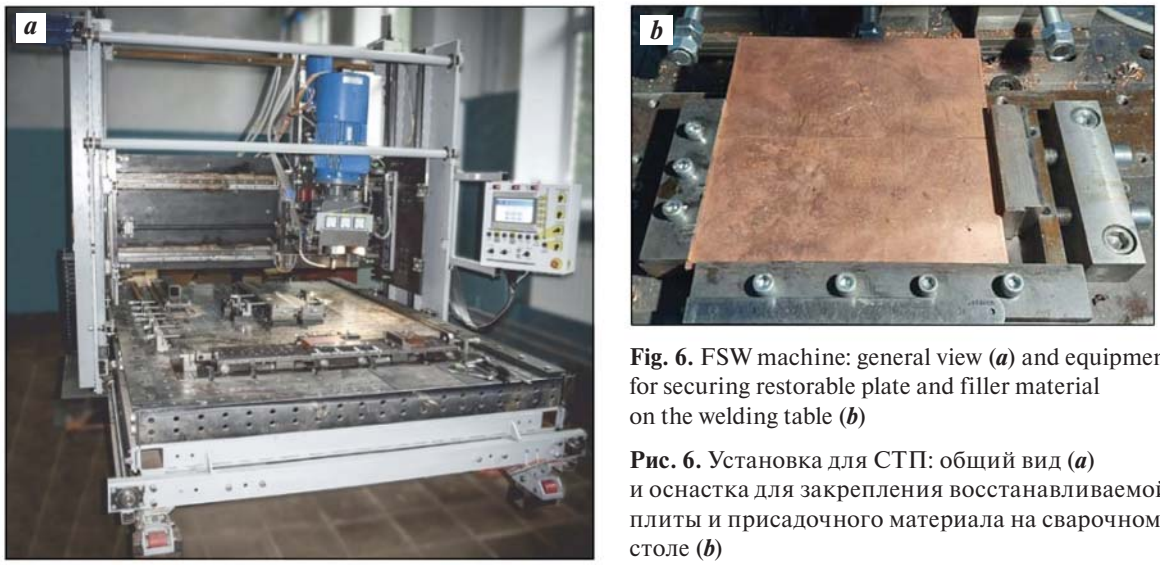

Fig. 6. FSW machine: general view (***a***) and equipment for securing restorable plate and filler material on the welding table (***b***)

Рис. 6. Установка для СТП: общий вид (***a***) и оснастка для закрепления восстанавливаемой плиты и присадочного материала на сварочном столе (***b***)

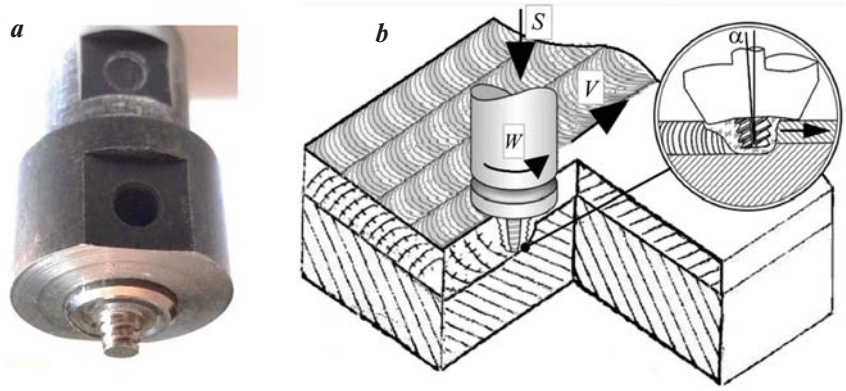

Fig. 7. Heat-resistant stir tool (***a***) and schematic drawing of multi-pass FSLW (***b***)
S – load, *W* – tool rotational speed, *V*– longitudinal welding velocity, α – tilt angle

Рис. 7. Внешний вид сварочного инструмента из жаропрочного сплава (***a***) и схема процесса плоскостной СТП (***b***)
S – нагрузка; *W* – скорость вращения инструмента, об/мин; *V* – скорость сварки, мм/мин; α – угол наклона, град

(tool) rotation speed $W = 900$ rpm, and welding speed V = 30 mm/min (refer to Fig. 7, *b*). Throughout the welding process, the parts were cooled by directing an air jet onto them. The temperature at the periphery of the tool shoulder was monitored using a DGE 10NV non-contact laser pyrometer (DIAS_Pyrospot, Germany).

Following FSW, a heat treatment procedure was implemented, involving quenching from 1050 °C (held for $\tau = 1$ hour in an evacuated ampoule) in water, followed by aging at $t = 450$ °C ($\tau = 1$ hour, cooled in air).

The macrostructure of the samples was examined through optical microscopy after etching in a 50 % aqueous solution of nitric acid. This analysis was conducted on transverse metallographic sections perpendicular to the passages of the welding tool. The fine structure was scrutinized using Transmission Electron Microscopy (TEM) using thin foils. For assessing hardness, a Vickers indenter with a load of 1 kg was employed via a Qness 10A+ automated hardness tester (Qness, Austria). Comprehensive data was obtained, including 2D maps, 3D hardness distribution profiles, and hardness distribution curves along the depth of the welded joint. This involved conducting 10 measurements at various depths to ascertain the hardness characteristics.

Results and discussion

Figure 8, *a* presents an overall view of the plate surface, which was reconstructed through multi-pass FSLW, displaying overlapped tracks from individual passes of the welding tool. The examination of the mac-

rostructure of the welded joint on a transverse section (across the passages) revealed specific characteristics (Fig. 8, *b*): the structure of the used bronze plate exhibited large recrystallized grains, measuring between 5 to 20 mm.

As documented in [39], scanning electron microscopy reveals spherical particles of pure chromium featuring a BCC lattice, measuring 1—5 μm in size, distributed within the grains of a metal matrix. Additionally, rod-shaped particles, reaching up to 1 μm in size and representing Cu_5Zr with a complex face-centered cubic lattice type Be_5Au [43], were observed. Optical microscopy (Fig. 9, *a*) also distinctly highlighted the presence of round chromium particles, up to 5 μm in size, within the plate's structure. Their existence in the original plate structure following hardening, aging, and prolonged operational use can be attributed to the limited solubility of chromium in copper, which, even at t = 1050 °C, does not exceed 0.6 wt.% [41].

Transmission electron microscopy observations revealed the existence of a specific quantity of dislocations within the copper grains (Fig. 10). However, the elevated hardness of the restored CCM mold plate, measuring between 116—126 HV1 (Fig. 11 and 12, curve *1*), is primarily attributed not only to these structural characteristics but predominantly to the presence of pre-deposits in the aged bronze, specifically Guinier—Preston zones, and nanodispersed chromium particles that are coherent with the matrix. These elements generate elastic stress fields within the matrix [44—46].

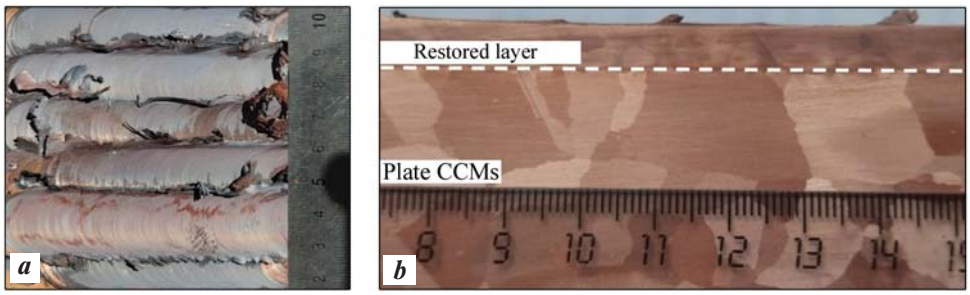

Fig. 8. Appearance of the FSW restored layer (***a***) and macrostructure of the restored layer and substrate in a transverse cross-section (***b***)

Рис. 8. Вид восстановленного СТП-слоя (***a***) и макроструктура восстановленного слоя и подложки в поперечном сечении (***b***)

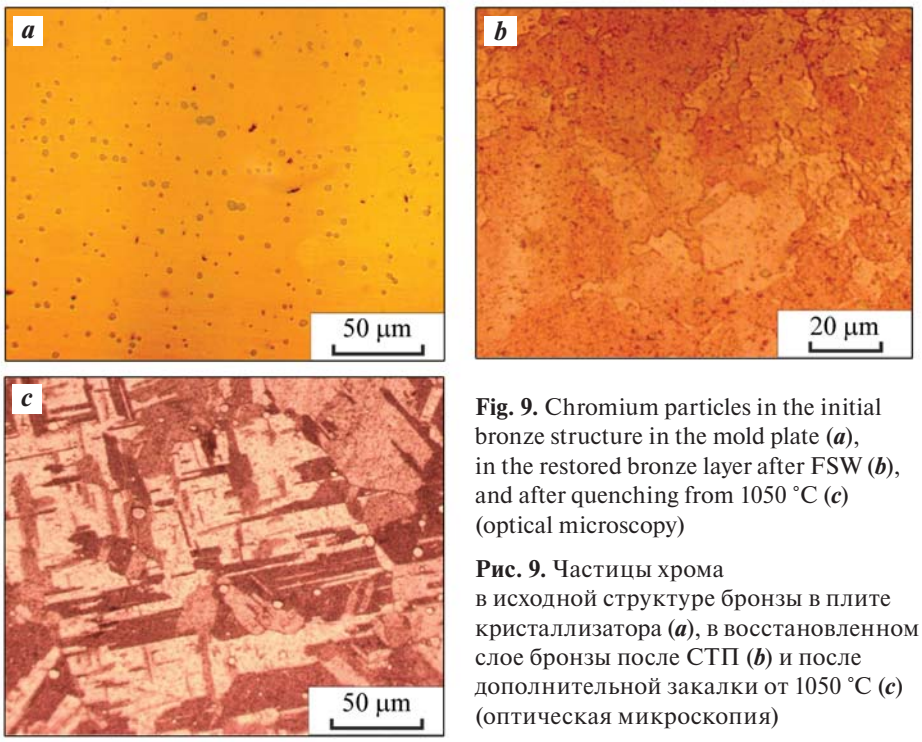

Fig. 9. Chromium particles in the initial bronze structure in the mold plate (***a***), in the restored bronze layer after FSW (***b***), and after quenching from 1050 °C (***c***) (optical microscopy)

Рис. 9. Частицы хрома в исходной структуре бронзы в плите кристаллизатора (***a***), в восстановленном слое бронзы после СТП (***b***) и после дополнительной закалки от 1050 °C (***c***) (оптическая микроскопия)

In Figure 8, *b*, it is evident that multi-pass welding, with a 6 mm step, generates a continuous bronze layer approximately 5 mm thick on the plate's surface. This layer is formed due to the partial overlap of welded joints. The restored layer exhibits a relatively uniform macrostructure. Importantly, no observable continuity defects such as breaks, cracks, or pores were detected either across the entire cross-section of the welded joint or along the boundary of the connection between the applied material and the metal of the plate undergoing restoration.

The analysis conducted via an automated hardness tester provided a 2D map, a 3D hardness distribution profile (Fig. 11), and a graph illustrating changes in hardness along the depth of the welded joint (Fig. 12, curve *1*). These assessments revealed a reduction in the hardness of the applied layer to a range of 85—105 HV1 due to multi-pass FSLW. This decrease contrasts with the initial hardness of the CCM mold plate, which was measured at 116—126 HV1. Additionally, no significant differences or noticeable drops in hardness were observed in the overlap area of adjacent passages. Within the thermomechanically affected zone (refer to Fig. 11, zone *II*), a slight increase in hardness was noted compared to the hardness level in the original (base) metal of the mold plate. This elevated hardness can be attributed to the deformation hardening of the plate material nearby the rotating welding tool caused by its mechanical action.

Optical metallography analysis reveals a notable dispersion in the structure of the deposited bronze layer, particularly evident in the weld nugget (Fig. 13). This dispersion results in the weld structure exhibiting grain sizes, ranging from units to tens of micrometers (Fig. 14). In the upper section of the layer restored by FSW (stir zone) (as shown in Fig. 13), a fine-grained equiaxial recrystallized structure emerges, characterized by a grain size of approximately 5 μm (refer to Fig. 14, *a*). While the predominant size of recrystallized grains in the stir zone falls within the range of

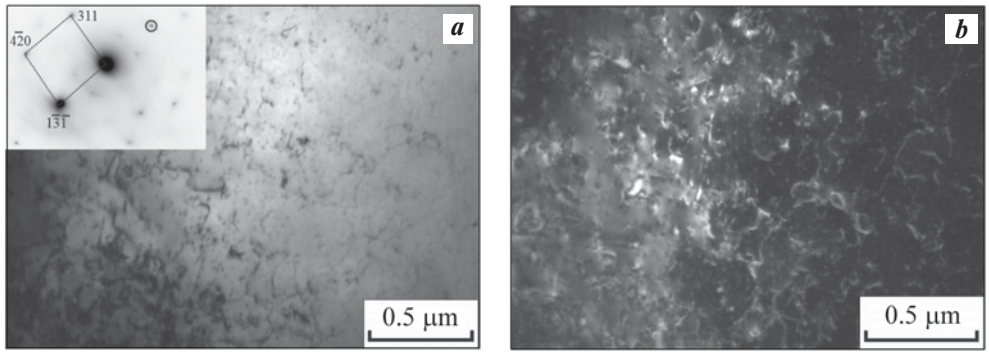

Fig. 10. Initial microstructure of the Cr–Zr bronze (TEM)
a – bright-field image and electron-diffraction pattern, zone axis [$12\bar{5}$]; ***b*** – dark-field image in the $\bar{1}31_{Cu}$ reflection

Рис. 10. Исходная структура бронзы из плиты кристаллизатора МНЛЗ (ПЭМ)
a – светлопольное изображение и картина микродифракции, ось зоны [$12\bar{5}$]; ***b*** – темнопольное изображение в рефлексе $\bar{1}31_{Cu}$

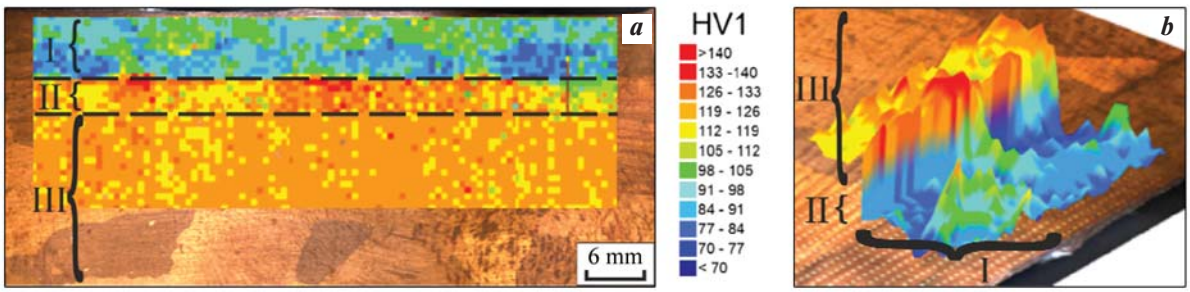

Fig. 11. Hardness distribution of the weld: 2D-map (***a***) and 3D profile (***b***)
I – stir zone of the restored layer; ***II*** – thermomechanically affected zone; ***III*** – initial (base) metal of the mold plate

Рис. 11. Распределение твердости по сечению сварного соединения: 2D-карта (***a***) и 3D-профиль (***b***)
I – восстановленный способом СТП слой бронзы (зона перемешивания); ***II*** – зона термомеханического влияния; ***III*** – исходный (основной) металл плиты кристаллизатора

5 to 15 μm, observations at different depths beneath the surface reveal areas and bands spanning several hundred micrometers with a grain size of up to 20—50 μm (see Fig. 14, *b*, *c*). Within the thermomechanically affected zone (refer to Fig. 13), a combination of fine-grained structure and deformed coarse grains is evident (depicted in Fig. 14, *d*). These areas gradually transition into the structure resembling the initial material of the mold plate.

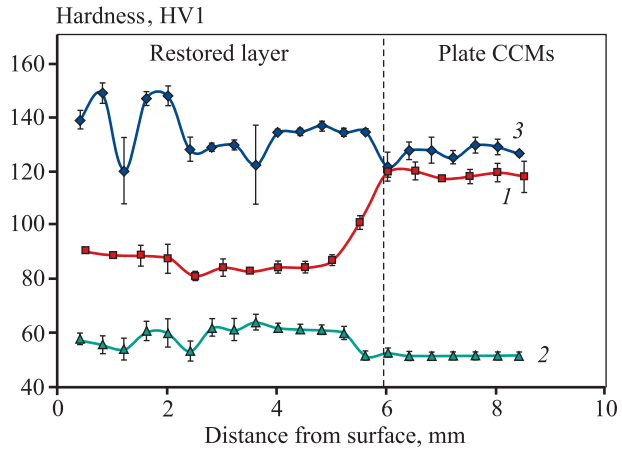

Fig. 12. Hardness distribution in the restored layer and the mold plate after various technological operations

1 – FSW; ***2*** – FSW + quenching 1050°C;
3 – FSW + quenching 1050°C + aging at 450°C

Рис. 12. Распределение твердости в восстановленном слое Cr–Zr-бронзы и плите кристаллизатора МНЛЗ после различных технологических операций

1 – СТП; ***2*** – СТП + закалка от 1050 °С;
3 – СТП + закалка от 1050 °С + старение при 450 °С

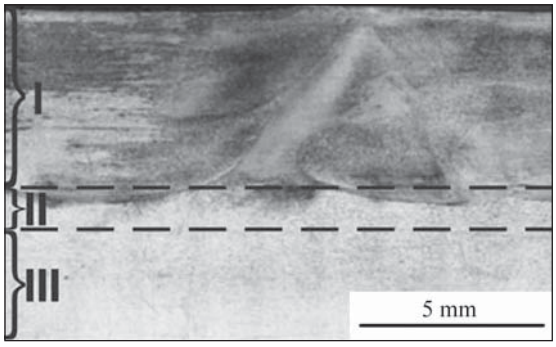

Fig. 13. General view of a transverse section of the weld

I – stir zone of the restored layer; ***II*** – thermomechanically affected zone; ***III*** – initial (base) metal of the mold plate

Рис. 13. Общий вид поперечного шлифа сварного соединения хромоциркониевой бронзы

I – восстановленный способом СТП слой (зона перемешивания);
II – зона термомеханического влияния;
III – исходный (основной) металл плиты кристаллизатора

The movement of material around the pin of the welding tool during FSW is intricate, characterized by gradients in the degree and rate of deformation as well as temperature fluctuations [18; 19]. Consequently, the microstructure in the weld nugget (stir zone) retains traces of varying thermomechanical histories of different metal layers. This leads to structural heterogeneity due to the complexity of FSW. In the case of multi-pass FSW (as shown in Fig. 7, *b* and 8, *a*), additional thermal and thermomechanical effects on the metal structure occur due to different weld zones overlapping (such as thermal and thermomechanically affected zones and the weld nugget). This further contributes to the observed structural heterogeneity in the restored layer and the zone of thermomechanical influence, as highlighted in Figs. 13 and 14. Notably, despite the varied grain sizes observed in these zones, it's essential to point out that this diversity did not significantly impact the uniformity of hardness distribution in these specified zones (as evident in Figs. 11 and 12). Furthermore, it's important to mention that the heat-affected zone does not exhibit distinct identification based on changes in the size of structural components or alterations in the material's hardness.

Transmission electron microscopy examinations in the stir zone reveal the presence of areas with deformed grains alongside a significant number of clean recrystallized grains characterized by broad banded boundaries (Fig. 15 *a*, *b*). Within these grains, chromium particles are observed (Fig. 15, *c*), with sizes that can extend up to 100 nm. Heating to high temperatures and intense plastic deformation during multi-pass FSW leads to the initiation of dynamic recrystallization processes behind the welding tool and contribute to the enlargement of strengthening phases (overaging). It's previously shown (refer to Fig. 9, *b*) that FSW does not result in complete dissolution of coarse chromium particles, which are initially present in the structure of the original plate (as seen in Fig. 9, *a*). Consequently, these relatively larger chromium particles, which can reach sizes of up to 5 μm, do not exert a decisive influence on the material's hardness.

The substantial decrease in hardness within the stir zone, from the initial 116—126 HV1 of the continuous caster mold plate to the range of 85—105 HV1 (as observed in Fig. 11 and 12), despite the significant refinement of the bronze grain structure (as depicted in Fig. 8, *b* and 14), is attributed to recrystallization and overaging processes resulting from multi-pass FSW. During the FSW of chromium zirconium bronze, the temperature measured at the periphery of the tool shoulder, composed of the heat-resistant alloy, registered at 500—550 °C (Fig. 16) using a non-contact laser pyrome-

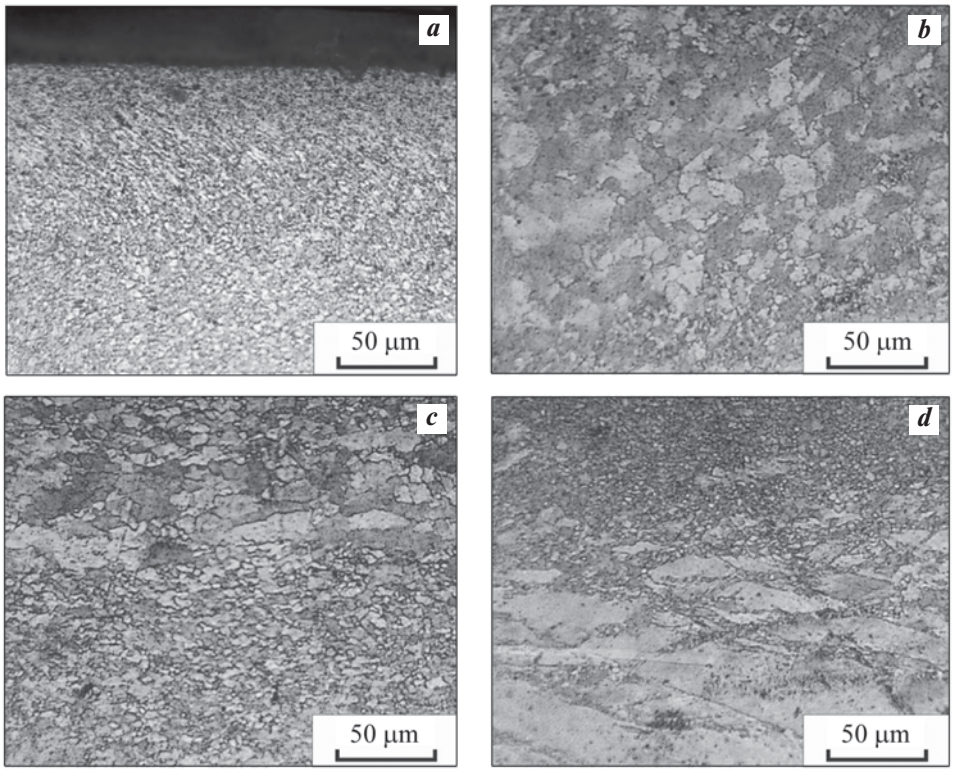

Fig. 14. Structure of chromium-zirconium bronze in the restored layer of the continuous caster mold plate after FSW (optical microscopy)

a – near the surface; ***b*** – mid area, ***c*** – area of variable grain structure, ***d*** – the transition zone «layer – base metal»

Рис. 14. Структура хромоциркониевой бронзы в восстановленном слое плиты кристаллизатора МНЛЗ после СТП (оптическая микроскопия)

a – вблизи поверхности; ***b*** – в центральной части восстановленного слоя, ***c*** – на границе участков с разноразмерной структурой, ***d*** – в переходной зоне с основным металлом

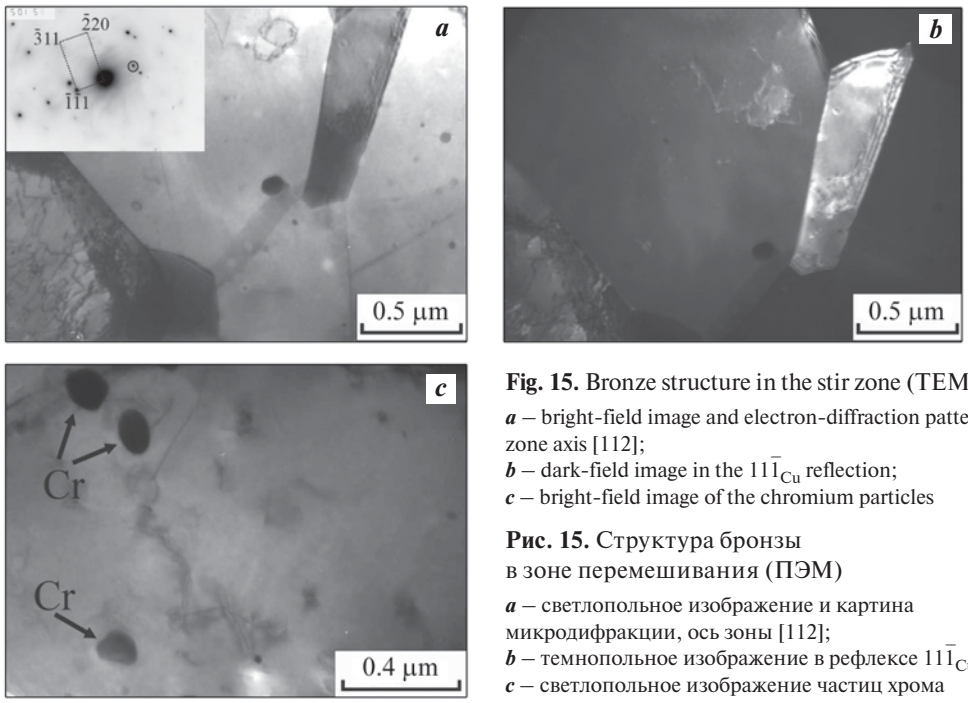

Fig. 15. Bronze structure in the stir zone (TEM)

a – bright-field image and electron-diffraction pattern, zone axis [112];
b – dark-field image in the $11\bar{1}_{Cu}$ reflection;
c – bright-field image of the chromium particles

Рис. 15. Структура бронзы в зоне перемешивания (ПЭМ)

a – светлопольное изображение и картина микродифракции, ось зоны [112];
b – темнопольное изображение в рефлексе $11\bar{1}_{Cu}$;
c – светлопольное изображение частиц хрома

ter. Simulation results [40] indicate that the temperature within the weld zone (stir zone) surpasses the measured value by 100—150 °C, reaching 600—700 °C. Additionally, the accumulation of metal heating under multi-pass FSW conditions contributes to the softening effect. In a study [39], during a single-pass FSW with a tool made of H13 die steel, which heated the welding zone to approximately 420 °C, a reduction in bronze softening was observed. Conversely, this led to material strengthening by 1.5—2.0 times. This outcome suggests that less heating did not trigger the development of overaging processes.

Quenching the material from 1050 °C induces substantial growth in many grains within the layer restored by multi-pass FSLW (Fig. 17, *a*, *b*). This growth occurs due to the development of recrystallization processes during high-temperature exposure to the quenching process. The thermal dissolution of dispersed strengthening phases, particularly chromium particles measuring up to 100 nm observed post-welding (refer to Fig. 15, *c*), facilitates the growth of recrystallized grains. Consequently, in certain areas of the restored layer, grain growth expands to several hundred microns, often accompanied by the formation of annealing twins (depicted in Fig. 17, *a*, *b*). The observed grain coarsening and the dissolution of dispersed reinforcing chromium particles contribute to significant softening, reducing

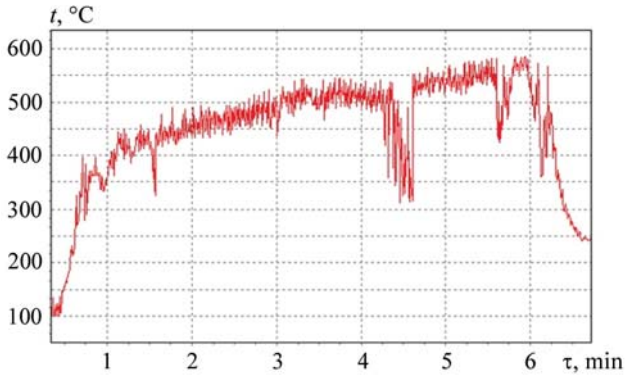

Fig. 16. Temperature variation at the periphery of the welding tool shoulder during FSW of Cr–Zr bronze

Рис. 16. Изменение температуры на периферии заплечика сварочного инструмента в процессе плоскостной СТП хромоциркониевой бронзы

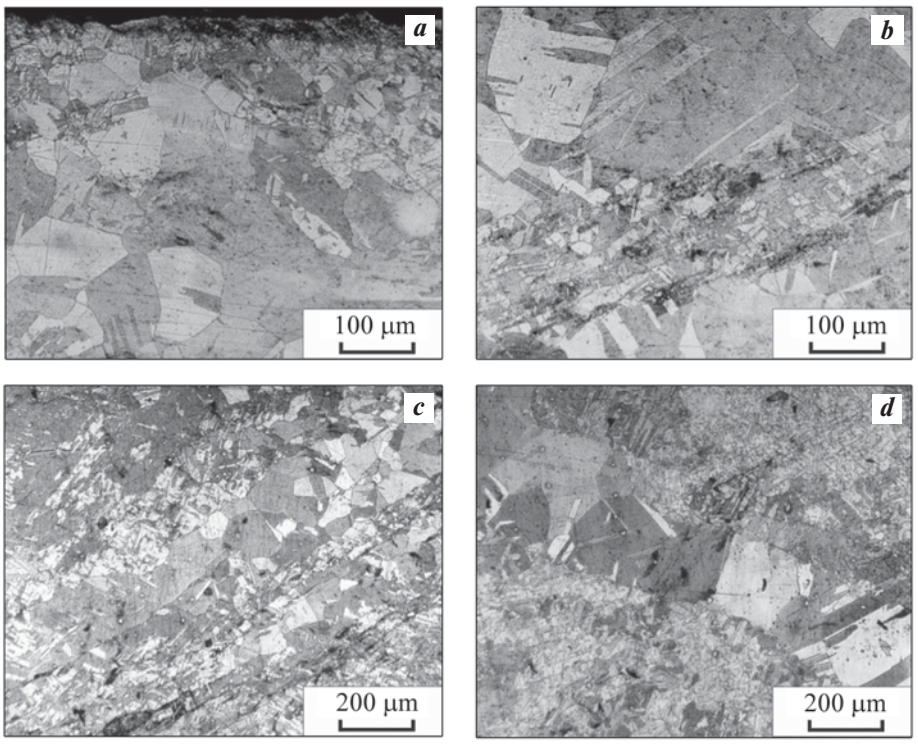

Fig. 17. Cr–Zr bronze structure in the restored layer after various heat treatments (optical microscopy)

a, ***b*** – FSW + quenching from 1050 °C; ***c***, ***d*** – FSW + quenching from 1050 °C + aging at 450 °C
a, ***c*** – near the surface; ***b***, ***d*** – in the mid area of the restored layer

Рис. 17. Структура хромоциркониевой бронзы в восстановленном слое плиты кристаллизатора МНЛЗ после различных термических обработок (оптическая микроскопия)

a, ***b*** – СТП + закалка от 1050 °C; ***c***, ***d*** – СТП + закалка от 1050 °C + старение при 450 °C
a, ***c*** – вблизи поверхности; ***b***, ***d*** – в центральной части восстановленного слоя

the hardness to values between 52—62 HV1, observed in both the restored layer with a dispersed structure and the coarse-grained base material of the plate (Fig. 12, curve *2*). Interestingly, even after one hour of hardening at t = 1050 °C, coarse chromium particles up to 5 microns in size, initially present in the bronze structure of the original plate (as seen in Fig. 9, *a*) and post-FSW treatment (as shown in Fig. 9, *b*), retain in the structure (seen in Fig. 9, *c*). This retention is due to the limited solubility of chromium in copper, which at the specified quenching temperature does not exceed 0.6 wt.% [41].

According to the observations made through transmission electron microscopy, following the quenching process, coarse grains exhibit a limited number of dislocations found both inside the grain and at high-angle boundaries (Fig. 18, *a*). Additionally, undissolved dispersed chromium particles, measuring up to 30 nm, are present (Fig. 18, *b*), alongside twins (Fig. 18, *c*, *d*). Figures 18, *c*, *d* also show a deformation contrast in the form of "butterfly wings" or arcs. The structural images reveal specific contrasts, such as "coffee beans" and "rings", which indicate the presence of Guinier—Preston zones within the structure. These zones are known to be coherently associated with the matrix [44; 45] or forming nuclei of chromium particles that generate a field of elastic stresses around themselves within the matrix [46]. The emergence of such characteristic structural features of aged bronze post-quenching in water [44—46] could be linked to the use of a sealed ampoule during the high-temperature heating of the sample, causing a delay in its cooling process.

Quenching followed by aging at t = 450 °C results in the strengthening of the weld joint to 120—150 HV1 (as observed in Fig. 12, curve *3*). This strengthening effect occurs despite the presence of large grains within the structure of the restored layer (seen in Fig. 17, *c*, *d*), formed during the heating to 1050 °C for quenching. In the bright-field TEM image, a contrast in the form of arcs is observed within the grain bulk (Fig. 19, *a*), indicating the initial stages of fine strengthening phase formation. Moreover, the dark-field image in Fig. 19, *b* indicates the release of a considerable number of dispersed particles enriched with chromium from a supersaturated solid solution. These released particles play a significant role in efficient dispersion strengthening, affecting both the layer restored by FSW and the origi-

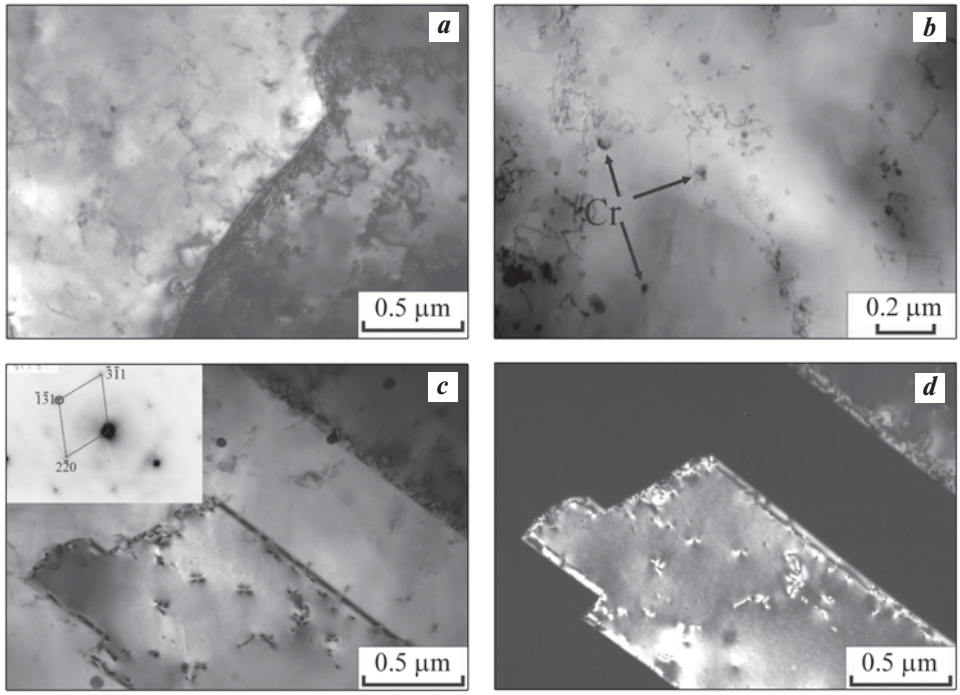

Fig. 18. Bronze structure in the stir zone of FSW joint at a depth of 1 mm (***a***, ***b***) and at a depth of 4 mm (***c***, ***d***) after quenching from 1050 °C (TEM)

a, ***b*** – bright-field images; ***c*** – bright-field image and electron-diffraction pattern, zone axis [114]; ***d*** – dark-field image in the $\bar{1}31_{Cu}$ reflection

Рис. 18. Структура бронзы в зоне перемешивания СТП на глубине 1 мм (***a***, ***b***) и 4 мм (***c***, ***d***) после закалки от 1050 °С (ПЭМ)

a, ***b*** – светлопольные изображения; ***c*** – светлопольное изображение и картина микродифракции, ось зоны [114], ***d*** – темнопольное изображение в рефлексе $\bar{1}31_{Cu}$

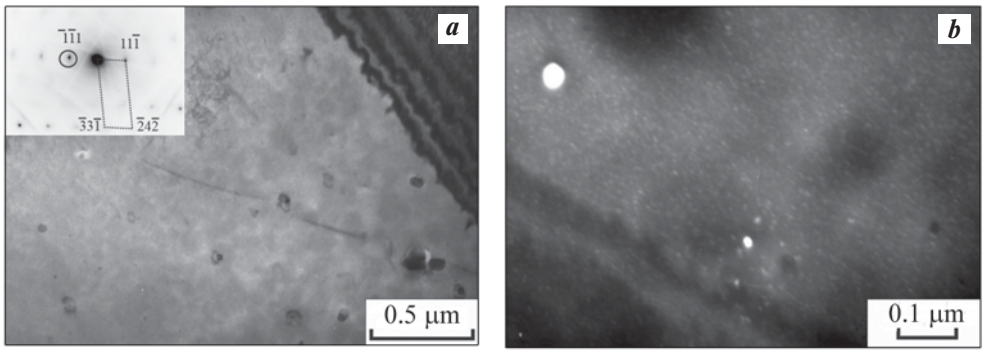

Fig. 19. Bronze structure in the stir zone near the surface at a depth of 1 mm, after quenching from 1050 °C followed by aging at 450 °C (TEM)

a – bright-field image and microdiffraction pattern, zone axis [123]; ***b*** – dark-field image in the $\bar{1}\bar{1}1_{Cu,Cr}$ mixed reflection

Рис. 19. Структура бронзы в зоне перемешивания СТП на глубине 1 мм после закалки от 1050 °С и старения при 450 °С (ПЭМ)

a – светлопольное изображение и картина микродифракции, ось зоны [123];
b – темнопольное изображения в смешанном рефлексе $\bar{1}\bar{1}1_{Cu,Cr}$

nal plate of chromium-zirconium bronze (as seen in Fig. 12, curve *3*). This signifies the dominant role of the dispersion strengthening mechanism over the grain boundary strengthening mechanism. Active release of dispersed chromium particles during aging is facilitated by the presence of chromium-enriched Guinier—Preston zones or chromium particle nuclei, as observed in the discussion regarding Fig. 18, *c*, *d*, subsequent to hardening. Consequently, this heat treatment process (quenching followed by aging) effectively reverses the de-strengthening effect observed in the stir zone of chromium-zirconium bronze, a result of overaging during the multi-pass FSW caused by overheating.

Conclusions

The manufacture and restoration of CCM molds hold significant strategic importance for ensuring the national safety of the Russian Federation within the steel industry. An innovative technology has been developed and practically implemented in major Russian metallurgical enterprises for the restoration and production of new mold plates, incorporating wear-resistant composite HVAF thermal spray coatings. This innovation has shown remarkable performance, surpassing imported plates with galvanic coatings by a significant margin (4—20 times), while simultaneously enhancing the quality of the produced workpieces. Consequently, the reliance on foreign slab molds in Russian metallurgical plants has been decreased from 97 % in 2012 to 40 % by the end of 2022.

To prolong the service life and reduce the cost of consumable components in a CCM, solutions are being sought to address the pressing issue of restoring copper plates of slab molds after reaching the minimum permissible thickness due to operation and repairs. The advantages and potential of restoring mold plates using Cr—Zr bronze are being explored, employing the environmentally friendly method of multi-pass Friction Stir Lap Welding by applying a filler plate made of the same material onto the restored plate. A series of successive passes using a rotating conical tool with partial joints overlap produced a welded layer (restored bronze layer) approximately 5 mm thick, exhibiting no critical continuity defects such as breaks, cracks, or pores. Various grain sizes, ranging from units to tens of microns, were observed in the weld zones.

The FSW process, coupled with blowing the welding zone with an air jet, resulted in softening of the bronze within the restored layer, measuring 85—105 HV1 compared to the original plate hardness of 116—126 HV1. This softening phenomenon is linked to dynamic recrystallization and overaging, involving the coarsening of chromium particles to approximately 100 nm in Cr—Zr bronze due to heating the weld nugget (stir zone) to temperatures of 600—700°C.

Subsequent quenching from 1050 °C further contributed to the softening of the bronze, reducing its hardness to 52—62 HV1. This affected both the FSW restored layer with a dispersed structure and the original plate containing coarse grains (5—20 mm) due to the development of recrystallization and thermal dissolution of dispersed strengthening phases (chromium particles) up to 100 nm in size, observed post-welding.

Subsequent aging at a t = 450 °C results in the strengthening of the restored layer to a 120—150 HV1,

despite the retention of coarse-grained structure formed during the heating process for quenching. This efficient strengthening during aging, observed in both the restored layer and the original plate, is attributed to the release of chromium-enriched dispersed particles from a supersaturated solid solution. This highlights the predominant role of the dispersion mechanism in strengthening Cr—Zr bronze over the grain-boundary strengthening mechanism. The active release of dispersed chromium particles during aging is facilitated by the formation of chromium-enriched Guinier—Preston zones or nuclei of chromium particles within the bronze layer restored by FSW, which begins during the quenching stage. Consequently, the softening of bronze during multi-pass FSW can be effectively eliminated by quenching followed by aging.

The restoration of copper plates to their original thickness using multi-pass friction stir lap welding coupled with the subsequent application of wear-resistant composite coatings ensures a continuous operational cycle for slab molds and substantially diminishes the necessity for their importation. The utilization of advanced FSW methods for plate restoration, apart from being economically efficient, also promises considerable environmental benefits. This approach reduces the requirement for environmentally harmful metallurgical production to manufacture new mold plates from copper alloys.

References

1. Kotelnikov A.V., Vopneruk A.A., Makarov A.V., Korobov Yu.S., Kirichkov A.A., Dagman A.I., Shefrin I.N. New materials and technologies for significantly increase the wear resistance of the working surface of metallurgical equipment. *Tyazheloe mashinostroenie*. 2018;(9):14—20. (In Russ.).
   Котельников А.Б., Вопнерук А.А., Макаров А.В., Коробов Ю.С., Киричков А.А., Дагман А.И., Шифрин И.Н. Новые материалы и технологии существенного повышения износостойкости рабочей поверхности металлургического оборудования. *Тяжелое машиностроение*. 2018;(9):14—20.
2. Vdovin K.N., Pozin A.E. Cavitation wear of coated copper walls of molds. *Stal'*. 2018;(9):14—20. (In Russ.).
   Вдовин К.Н., Позин А.Е. Кавитационный износ медных стенок кристаллизаторов с покрытием. *Сталь*. 2017;(3):49—51.
3. Kushnarev A.V., Kirichkov A.A., Vopneruk A.A., Kotelnikov A.V., Korobov Yu.S., Makarov A.V., Filatov S.V., Shefrin I.N. Physico-mechanical characteristics of thermal sprayed coatings on the walls of the mold of continuous casting machines. *Svarka i diagnostika*. 2017;(5):50—53. (In Russ.).
   Кушнарев А.В., Киричков А.А., Вопнерук А.А., Котельников А.Б., Коробов Ю.С., Макаров А.В., Филатов С.В., Шифрин И.Н. Физико-механические характеристики газотермических покрытий стенок кристаллизатора машин непрерывного литья заготовок. *Сварка и диагностика*. 2017;(5):50—53.
4. Korobov Yu.S., Kotelnikov A.B., Kushnarev A.V., Kirichkov A.A., Filippov M.A., Vopneruk A.A. Analysis of the features of the formation of thermal sprayed coatings on the wall slab crystallizer. *Chernye metally*. 2017;(1): 41—45. (In Russ.).
   Коробов Ю.С., Котельников А.Б., Кушнарев А.В., Киричков А.А., Филиппов М.А., Вопнерук А.А. Анализ особенностей формирования газотермических покрытий на стенке слябового кристаллизатора. *Черные металлы*. 2017;(1):41—45.
5. Makarov A.V., Soboleva N.N., Malygina I.Yu. Role of the strengthening phases in abrasive wear resistance of laser-clad NiCrBSi coatings. *Journal of Friction and Wear*. 2017;38(4): 272—278.
   Макаров А.В., Соболева Н.Н., Малыгина И.Ю. Роль упрочняющих фаз в сопротивлении абразивному изнашиванию NiCrBSi покрытий, сформированных лазерной наплавкой. *Трение и износ*. 2017;38(4): 311—318.
6. Makarov A.V., Soboleva N.N., Malygina I.Yu., Osintseva A.L. Possibility of obtaining heat-resistant coating: Patent 2492980 (RF). 2013. (In Russ.).
   Макаров А.В., Соболева Н.Н., Малыгина И.Ю., Осинцева А.Л. Способ получения теплостойкого покрытия: Патент 2492980 (РФ). 2013.
7. Makarov A.V., Soboleva N.N., Malygina I.Yu., Osintseva A.L. Formation of wear-resistant chromium-nickel coating with extra high thermal stability by combined laser-and-heat treatment. *Metal Science and Heat Treatment*. 2015;57(3-4):161—168.
   Макаров А.В., Соболева Н.Н., Малыгина И.Ю., Осинцева А.Л. Формирование износостойкого хромоникелевого покрытия с особо высоким уровнем теплостойкости комбинированной лазерно-термической обработкой. *Металловедение и термическая обработка металлов*. 2015;(3):39—46.
8. Makarov A.V., Soboleva N.N., Malygina I.Yu., Kharanzhevskiy E.V. Improving the properties of a rapidly crystallized NiCrBSi laser clad coating with high-temperature processing. *Journal of Crystal Growth*. 2019;525;125200.
   https://doi.org/10.1016/j.jcrysgro.2019.125200
9. Soboleva N.N., Makarov A.V. Effect of conditions of high-temperature treatment on the structure and tribological

properties of nickel-based laser-clad coating. *Russian Journal of Non-Ferrous Metals*. 2021;62(6): 682—691. https://link.springer.com/article/10.3103/S1067821221060183
Соболева Н.Н., Макаров А.В. Влияние условий высокотемпературной обработки на структуру и трибологические свойства наплавленного лазером покрытия на никелевой основе. *Известия вузов. Цветная металлургия*. 2021;27(5):67—77. https://doi.org/10.17073/0021-3438-2021-5-67-77
10. Gurevich S.M. Handbook on welding of non-ferrous metals. Kiev: Naukova dumka, 1981. 608 p.
Гуревич С.М. Справочник по сварке цветных металлов. Киев: Наукова думка, 1981. 608 p. (In Russ.).
11. Kazakov N.F. Diffusion Bonding of Materials. Oxford, New York: Pergamon Press, 1985. 304 p.
12. Lysak V., Kuzmin S. Lower boundary in metal explosive welding. Evolution of ideas. *Journal of Materials Processing Technology*. 2012;212(1):150—156. https://doi.org/10.1016/j.jmatprotec.2011.08.017
13. Nazarov A.A., Murzinova M.A., Mukhametgalina A.A., Shayakhmetova E.R. Bulk ultrasonic treatment of crystalline materials. *Metals*. 2023;13(2):344. https://doi.org/10.3390/met13020344
14. Sun F., Liu P., Chen X., Zhou H., Guan P., Zhu B., Mechanical properties of high-strength Cu—Cr—Zr alloy fabricated by selective laser melting. *Materials*. 2020;13;5028. https://doi.org/10.3390/ma13215028
15. Tang X., Chen X., Sun F., Liu P., Zhou H., Fu S. The current state of CuCrZr and CuCrNb alloys manufactured by additive manufacturing: A review. *Materials & Design*. 2022;224;111419. https://doi.org/10.1016/j.matdes.2022.111419
16. Klimenko Yu.V. Method of friction welding of metals: Patent 195846 (USSR). 1967. (In Russ.).
Клименко Ю.В. Способ сварки металлов трением: Патент 195846 (СССР). 1967.
17. Thomas W.M., Nicholas E.D., Needham J.C., Murch M.G., Templesmith P., Dawes C.J. Optimization of welding parameters for friction stir lap welding of AA6061-T6 alloy: Patent PCT/GB92/02203 (International).1991.
18. Mishra R.S., Ma Z.Y. Friction stir welding and processing. *Materials Science and Engineering: R*. 2005;50(1-2):1—78. https://doi.org/10.1016/j.mser.2005.07.001
19. Mishra R.S., Mahoney M.W. Friction stir welding and processing. *ASM International*. 2007;1:1—5. https://doi.org/10.1361/fswp2007p001
20. Heidarzadeh A., Mironov S., Kaibyshev R., Çam G., Simar A., Gerlich A., Khodabakhshi F., Mostafaei A., Field D.P., Robson J.D., Deschamps A., Withers P.J. Friction stir welding/processing of metals and alloys: A comprehensive review on microstructural evolution. *Progress in Materials Science*. 2021;(117):100752. https://doi.org/10.1016/j.pmatsci.2020.100752
21. Lee W.B., Jung S.B. The joint properties of copper by friction stir welding. *Materials Letters*. 2004;58(6): 1041—1046. https://doi.org/10.1016/j.matlet.2003.08.014
22. Sun Y.F., Fujii H. Investigation of the welding parameter dependent microstructure and mechanical properties of friction stir welded pure copper. *Materials Science and Engineering: A*. 2010;527(26):6879—6886. https://doi.org/10.1016/j.msea.2010.07.030
23. Surekha K., Els-Botes A. Development of high strength, high conductivity copper by friction stir processing. *Materials & Design*. 2011;32(2)911—916. https://doi.org/10.1016/j.matdes.2010.08.028
24. Palko W.A., Fielder R.S., Young P.F. Investigation of the use of friction stir processing to repair and locally enhance the properties of large NiAl bronze propellers. *Materials Science Forum*. 2003;426-432:2909—2914. https://doi.org/10.4028/www.scientific.net/MSF.426-432.2909
25. Oh-Ishi K., Zhilyaev A.P., McNelley T.R. A microtexture investigation of recrystallization during friction stir processing of as-cast NiAl bronze. *Metallurgical and Materials Transactions A*. 2006;37(7):2239—2251. https://doi.org/10.1007/BF02586143
26. Barlas Z., Uzun H. Microstructure and mechanical properties of friction stir butt welded dissimilar Cu/CuZn30 sheets. *Journal of Achievements in Materials and Manufacturing Engineering*. 2008;30(2):182—186.
27. Heidarzadeh A. Saeid T., Klemm V., Chabok A., Pei Y. Effect of stacking fault energy on the restoration mechanisms and mechanical properties of friction stir welded copper alloys. *Materials & Design*. 2019;162:185—197. https://doi.org/10.1016/j.matdes.2018.11.050
28. Galvão I., Loureiro A., Rodrigues D. M. Critical review on friction stir welding of aluminium to copper. *Science and Technology of Welding and Joining*. 2016;21(7):523—546. https://doi.org/10.1080/13621718.2015.1118813
29. Zoeram A.S., Anijdan S.H.M., Jafarian H.R., Bhattacharjee T. Welding parameters analysis and microstructural evolution of dissimilar joints in Al/Bronze processed by friction stir welding and their effect on engineering tensile behavior. *Materials Science and Engineering: A*. 2017;687:288—297. https://doi.org/10.1016/j.msea.2017.01.071
30. Narasimharaju S., Sankunny S. Microstructure and fracture behavior of friction stir lap welding of dissimilar AA 6060-T5/Pure copper. *Engineering Solid Mechanics*. 2019;7(3):217—228. https://doi.org/10.5267/j.esm.2019.5.002

31. Avettand-Fènoël M.N., Nagaoka T., Marinova M., Taillard R. Upon the effect of Zn during friction stir welding of aluminum-copper and aluminum-brass systems. *Journal of Manufacturing Processes*. 2020;58: 259—278. https://doi.org/10.1016/j.jmapro.2020.08.006
32. Ni D.R., Xiao B.L., Ma Z.Y., Qiao Y.X., Zheng Y.G. Corrosion properties of friction—stir processed cast NiAl bronze. *Corrosion Science*. 2010;52(5):1610—1617. https://doi.org/10.1016/j.corsci.2010.02.026
33. Li Y., Lian Y., Sun Y. Cavitation erosion behavior of friction stir processed nickel aluminum bronze. *Journal of Alloys and Compounds*. 2019;795:233—240. https://doi.org/10.1016/j.jallcom.2019.04.302
34. Lv Y., Nie B., Wang L., Cui H., Li L., Wang R., Lyu F. Optimal microstructures on fatigue properties of friction stir processed NiAl bronze alloy and its resistant fatigue crack growth mechanism. *Materials Science and Engineering: A*. 2020;771:138577. https://doi.org/10.1016/j.msea.2019.138577
35. He D.Q., Lai R.L., Xu Sh.H., Yang K.Y., Ye Sh.Y., Wang J., Zhu J.M., Suet B. Microstructure and mechanical properties of Cu—Cr—Zr alloy by friction stir welding. *Advanced Materials Research*. 2012;602-604:608—611. https://doi.org/10.4028/www.scientific.net/AMR.602-604.608
36. Wang Y.D., Zhu S.Z., Xie G.M., Wu L.H., Xue P., Ni D.R., Xiao B.L., Ma Z.Y. Realising equal-strength welding with good conductivity in Cu—Cr—Zr alloy via friction stir welding. *Science and Technology of Welding and Joining*. 2021;26(6):448—454. https://doi.org/10.1080/13621718.2021.1935151
37. Nikityuk Yu.N., Grigorenko G.M., Zelenin V.I., Zelenin E.V., Poleshchuk M.A. Technology for the restoration of slab molds of continuous casters using friction stir surfacing. *Sovremennaya elektrometallurgiya*. 2013;(3): 51—55. (In Russ.).
Никитюк Ю.Н., Григоренко Г.М., Зеленин В.И., Зеленин Е.В., Полещук М.А. Технология восстановительного ремонта слябовых кристаллизаторов МНЛЗ способом наплавки трением с перемешиванием. *Современная электрометаллургия*. 2013;(3):51—55.
38. Grigorenko G.M., Adeeva L.I., Tunik A.Yu., Poleshchuk M.A., Zelenin V.I., Zelenin E.V. Refurbishment of slab copper crystallizers of continuous casting machines. Structure and properties of metal in the joint zone. *Sovremennaya elektrometallurgiya*. 2015;(1):44—49.
Григоренко Г.М., Адеева Л.И., Туник А.Ю., Полещук М.А., Зеленин В.И., Зеленин Е.В. Восстановительный ремонт слябовых медных кристаллизаторов МНЛЗ. Структура и свойства металла в зоне соединения. *Современная электрометаллургия*. 2015;(1):44—49.
39. Lezhnin N.V., Makarov A.V., Volkova E.G., Valiullin A.I., Kotelnikov A.B., Vopneruk A.A. Realizing ultrafine grain structure of Cu—Cr—Zr alloy via friction stir welding/processing. *Letters on Materials*. 2022;12(4):428—432. https://doi.org/10.22226/2410-3535-2022-4-428-432
40. Lai R., Li X., He D., Lin J., Li J., Lei Q. Microstructures evolution and localized properties variation of a thick friction stir welded CuCrZr alloy plate. *Journal of Nuclear Materials*. 2018;510;70—79. https://doi.org/10.1016/j.jnucmat.2018.07.055
41. Osintsev O.E., Fedorov V.N. Copper and copper alloys. Domestic and foreign brands: Directory. 2nd ed., revised. and additional Moscow: Innovatsionnoe mashinostroenie, 2016. 360 p. (In Russ.).
Осинцев О.Е., Федоров В.Н. Медь и медные сплавы. Отечественные и зарубежные марки: Справочник. 2-е изд., перераб. и доп. М.: Инновационное машиностроение, 2016. 360 с.
42. Morozova A., Mishnev R., Belyakov A., Kaibyshev R. Microstructure and properties of fine grained Cu—Cr—Zr alloys after termo-mechanical treatments. *Reviews on Advanced Materials Science*. 2018;54;56—92. https://doi.org/10.1515/rams-2018-0020
43. Khomskaya I.V., Zel'dovich V.I., Frolova N.Y., Abdullina D.N., Kheifets A.E. Investigation of Cu_5Zr particles precipitation in Cu—Zr and Cu—Cr—Zr alloys subjected to quenching and high strain rate deformation. *Letters on Materials*. 2019;9(4):400—404. https://doi.org/10.22226/2410-3535-2019-4-400-404
44. Edwards D.J., Singh B.N., Tähtinen S. Effect of heat treatments on precipitate microstructure and mechanical properties of a CuCrZr alloy. *Journal of Nuclear Materials*. 2007;367-370:904—909. https://doi.org/10.1016/j.jnucmat.2007.03.064
45. Park J.-Y., Lee J.-S., Choi B.-K., Hong B.G., Jeong Y.H. Effect of cooling rate on mechanical properties of aged ITER-grade CuCrZr. *Fusion Engineering and Design*. 2008;83:1503—1507. https://doi.org/10.1016/j.fusengdes.2008.07.006
46. Zel'dovich V.I., Khomskaya I.V., Frolova N.Yu., Kheifets A.E., Shorokhov E.V., Nasonov P.A. Structure of chromium-zirconium bronze subjected to dynamic channel-angular pressing and aging. *Physics of Metals and Metallography*. 2013;114(5):411—418. https://doi.org/10.1134/S0031918X13050141
Зельдович В.И., Хомская И.В., Фролова Н.Ю., Хейфец А.Э, Шорохов Е.В., Насонов П.А. Структура хромоциркониевой бронзы, подвергнутой динамическому канально-угловому прессованию и старению. *Физика металлов и металловедение*. 2013;114(5):449—456. https://doi.org/10.7868/S0015323013050148

Information about the authors

Alexey V. Makarov – Dr. Sci. (Eng.), Corresponding Member of RAS, Head of Materials Science Department, Head of Mechanical Properties Laboratory, M.N. Miheev Institute of Metal Physics of Ural Branch of the Russian Academy of Sciences (IMP UB RAS).
https://orcid.org/0000-0002-2228-0643
E-mail: av-mak@yandex.ru

Nikita V. Lezhnin – Cand. Sci. (Eng.), Senior Research Scientist of Mechanical Properties Laboratory, IMP UB RAS.
https://orcid.org/0000-0001-9483-6607
E-mail: nlezhnin@bk.ru

Alexander B. Kotelnikov – General Director of CJSC Scientific and Production Enterprise «Mashprom".
https://orcid.org/0009-0005-9471-9378
E-mail: office@mashprom.ru

Alexander A. Vopneruk – Cand. Sci. (Eng.), Project Manager of CJSC Scientific and Production Enterprise "Mashprom".
https://orcid.org/0000-0002-0179-5453
E-mail: vopneruk@gmail.com

Yuri S. Korobov – Dr. Sci. (Eng), Chief Research Scientist, Head of Laboratory of Laser and Plasma Processing, IMP UB RAS; Professor of the Department of Welding Production Technology, Ural Federal University named after the First President of Russia B.N. Yeltsin.
https://orcid.org/0000-0003-0553-918X
E-mail: yukorobov@imp.uran.ru

Andrey I. Valiullin – Cand. Sci. (Eng.), Research Scientist of Mechanical Properties Laboratory, IMP UB RAS.
https://orcid.org/0000-0001-5539-4295
E-mail: a_valiullin@mail.ru

Elena G. Volkova – Cand. Sci. (Phys.-Math.), Senior Research Scientist of Mechanical Properties Laboratory, IMP UB RAS.
https://orcid.org/0000-0003-4958-3027
E mail: volkova@imp.uran.ru

Информация об авторах

Алексей Викторович Макаров – д.т.н., чл.-корр. РАН, гл. науч. сотрудник, зав. отделом материаловедения и лабораторией механических свойств Института физики металлов им. М.Н. Михеева Уральского отделения Российской академии наук (ИФМ УрО РАН).
https://orcid.org/0000-0002-2228-0643
E-mail: av-mak@yandex.ru

Никита Владимирович Лежнин – к.т.н., ст. науч. сотрудник лаборатории механических свойств ИФМ УрО РАН.
https://orcid.org/0000-0001-9483-6607
E-mail: nlezhnin@bk.ru

Александр Борисович Котельников – ген. директор ЗАО «НПП "Машпром"».
https://orcid.org/0009-0005-9471-9378
E-mail: office@mashprom.ru

Александр Александрович Вопнерук – к.т.н., руководитель проекта ЗАО «НПП "Машпром"».
https://orcid.org/0000-0002-0179-5453
E-mail: vopneruk@gmail.com

Юрий Станиславович Коробов – д.т.н., гл. науч. сотрудник, зав. лабораторией лазерной и плазменной обработки ИФМ УрО РАН; профессор кафедры технологии сварочного производства Уральского федерального университета имени первого Президента России Б.Н. Ельцина.
https://orcid.org/0000-0003-0553-918X
E-mail: yukorobov@imp.uran.ru

Андрей Илдарович Валиуллин – к.т.н., науч. сотрудник лаборатории механических свойств ИФМ УрО РАН.
https://orcid.org/0000-0001-5539-4295
E-mail: a_valiullin@mail.ru

Елена Георгиевна Волкова – к.ф.-м.н., ст. науч. сотрудник лаборатории механических свойств ИФМ УрО РАН.
https://orcid.org/0000-0003-4958-3027
E mail: volkova@imp.uran.ru

Contribution of the authors

A.V. Makarov – conceptualized and defined the work's objectives, wrote the manuscript.

N.V. Lezhnin – conducted sample welding, prepared thin sections, conducted optical microscopy, and contributed to defining the work's objectives and discussing the results.

A.B. Kotelnikov – contributed to defining the work's objectives and discussing the results.

A.A. Vopneruk – contributed to defining the work's objectives and discussing the results

Yu.S. Korobov – Contributed to manuscript writing.

A.I. Valiullin – conducted microhardness measurements and assisted in data plotting.

E.G. Volkova – conducted transmission electron microscopy.

Вклад авторов

А.В. Макаров – определение цели работы, написание статьи.

Н.В. Лежнин – сварка образцов, подготовка шлифов, проведение оптической микроскопии, участие в определении цели работы и обсуждении результатов.

А.Б. Котельников – участие в определении цели работы и обсуждении результатов.

А.А. Вопнерук – участие в определении цели работы и обсуждении результатов.

Ю.С. Коробов – участие в написании текста статьи.

А.И. Валиуллин – измерение микротвердости, построение графиков.

Е.Г. Волкова – проведение просвечивающей электронной микроскопии.

The article was submitted 20.10.2023, revised 06.11.2023, accepted for publication 10.11.2023

Статья поступила в редакцию 20.10.2023, доработана 06.11.2023, подписана в печать 10.11.2023